Eur. Phys. J. D (2014) 68: 354
DOI: 10.1140/epjd/e2014-50442-6

THE EUROPEAN
PHYSICAL JOURNAL D

Regular Article

Laser-assisted ionization-excitation of helium by electron impact at large momentum transfer

Andrey A. Bulychev[1,a] and Konstantin A. Kouzakov[2]

[1] Laboratory of Theoretical Physics, Joint Institute for Nuclear Research, Moscow Region, 141980 Dubna, Russia
[2] Department of Nuclear Physics and Quantum Theory of Collisions, Faculty of Physics, Lomonosov Moscow State University, 119991 Moscow, Russia

Received 10 June 2014 / Received in final form 26 August 2014
Published online 25 November 2014 –

Abstract. Ionization of a helium atom by electron impact in the presence of laser radiation is studied theoretically. The kinematic regime of high impact energy and large momentum transfer is considered. The S-matrix of the process is treated within the first Born and binary-encounter approximations. Triple differential cross sections are calculated for the cases when the residual He^+ ion is left both in the ground ($n = 1$) and in the first excited ($n = 2$) states in the presence of a laser field with frequency $\omega = 1.55$ eV and intensity $I = 5 \times 10^{11}$ W/cm^2. The laser-assisted cross sections corresponding to $n = 2$ are found to be more sensitive to the electron-electron correlations in helium than the field-free ones.

1 Introduction

The $(e, 2e)$ method at high impact energy and large momentum transfer, also known as electron momentum spectroscopy (EMS), is a powerful tool for exploring the electron momentum distribution in atoms, molecules, clusters, and solids (see Refs. [1–3] and references therein). The key feature of EMS is the kinematics of quasielastic knockout of the target electron by a fast incoming electron. This is realized under high-energy Bethe ridge conditions, when the energy and momentum transferred to the target are absorbed by the ejected electron. Describing the fast incoming and outgoing electrons by plane waves and involving the first Born approximation, one finds the fully differential cross section (FDCS) to be proportional to the momentum density of the ionized electron orbital $|\psi(\boldsymbol{q})|^2$ (the Kohn-Sham orbital [2]), with $-\boldsymbol{q}$ being equal to the recoil-ion momentum. The shape of the FDCS as a function of kinematical variables depends strongly only on $\boldsymbol{q}$ and for this reason it is usually called the momentum profile [2].

The advance in laser technologies stimulates laser applications in various fields of atomic physics [4]. In particular, Höhr et al. [5,6] recently carried out the first kinematically complete $(e, 2e)$ measurements on helium in the presence of laser radiation. Theoretical investigations of laser-assisted atomic ionization by electron impact began in the 1980s. A number of results concerning the dependence of the cross sections on laser-field parameters, such as polarization, frequency and intensity, have been obtained (see Refs. [7,8] for a review and also more recent articles [9–15]). Most of these works were focused on coplanar asymmetric kinematics involving small momentum transfer, whereas the theoretical studies for the case of the EMS kinematics have appeared only very recently [16–18]. At the present stage, an apparatus for $(e, 2e)$ EMS has been developed which, in combination with a sufficiently high intensity laser, lends an opportunity for conducting laser-assisted EMS measurements [19].

The first theoretical analysis of the laser-assisted EMS method [16] was carried out for the case of atomic hydrogen, which is a benchmark system for EMS. However, from the viewpoint of experimental realization, a helium atomic target is more convenient and "easy-to-use". Field-free EMS experiments on helium [20–22] show that momentum profiles are practically insensitive to the employed model of the target wave function if the residual He^+ ion remains in the ground state after the collision. In contrast, ionization-excitation processes, that is, those where the He^+ ion is left in an excited state, appear to be very sensitive to the electron-electron correlation in the He wave function. In this connection, it is interesting to examine whether or not such sensitivity remains in the presence of the laser field as well. Laser-assisted $(e, 2e)$ processes of helium were treated theoretically in earlier studies [6,9,14,23,24]. In those works however, no attention was paid to the role of the He wave function, and the ionization-excitation processes were not discussed. Therefore, in the present work, we study theoretically the laser-assisted EMS of helium, mainly focusing on ionization-excitation processes (clearly, such processes are absent in the hydrogen case discussed in Ref. [16]).

The paper is organized as follows. Section 2 delivers a theoretical framework for the laser-assisted EMS of helium. In Section 3, numerical results for laser-assisted momentum profiles of helium are presented and discussed. The conclusions are drawn in Section 4.

[a] e-mail: bulychev@theor.jinr.ru

2 Theory

We consider the case of a linearly polarized laser wave with frequency ω and a wave vector $\boldsymbol{k}$ ($k = \omega/c$). A typical situation is when the laser wavelength $\lambda = 2\pi/k$ is much greater than the spatial extent both of the target and of the region where the electron-electron collision takes place. This validates the use of the dipole approximation for the electric component and vector potential of the laser field, respectively,

$$\boldsymbol{F}(t) = \boldsymbol{F}_0 \cos\omega t, \qquad \boldsymbol{A}(t) = -\frac{c}{\omega}\boldsymbol{F}_0 \sin\omega t.$$

In order to discard possible photoionization effects, the electric-field amplitude F_0 and the field frequency ω are supposed to be small on the atomic scale, so that the Keldysh parameter [25] is $\gamma \gg 1$. In what follows, the incident, scattered and ejected electron energies and momenta are specified by respectively $(E_0, \mathbf{p}_0)$, $(E_s, \mathbf{p}_s)$ and $(E_e, \mathbf{p}_e)$.

Using the first Born and binary-encounter approximations, the S-matrix for the laser-assisted EMS process is evaluated as [16]

$$S = -i \int_{-\infty}^{\infty} dt \langle \chi_{\boldsymbol{p}_s}(t)\chi_{\boldsymbol{p}_e}(t)\psi_f(t)\,|v_{ee}|\,\chi_{\boldsymbol{p}_0}(t)\psi_i(t)\rangle, \quad (1)$$

where $\chi_{\boldsymbol{p}}$ stands for the incoming and outgoing electron states, $\psi_{i(f)}$ is the laser-dressed initial atomic (final ionic) state, and v_{ee} is the Coulomb potential between the colliding electrons. The validity of expression (1) is restricted to the kinematical regime of high impact energy and large momentum transfer. In addition, the value of the momentum

$$\boldsymbol{q} = \boldsymbol{p}_s + \boldsymbol{p}_e - \boldsymbol{p}_0$$

is supposed to be much smaller than p_0, p_s, and p_e and to lie in the range of momentum values typical for atomic electrons.

Clearly, the S-matrix is gauge-invariant. However, this property can be violated if one uses approximate treatments, for example, such as time-dependent perturbation theory, when accounting for the laser-field effect on electron states. In what follows, we employ the length (or electric-field) gauge, which gives more accurate perturbation results for laser-modified target states than the velocity (or Coulomb) gauge (see Refs. [18,26]).

The incoming and outgoing electron states are described in terms of Volkov functions [27], which are solutions to the Schrödinger equation for the electron motion in a plane electromagnetic wave. In the length gauge, the Volkov solution reads [28]

$$\chi_{\boldsymbol{p}}(\boldsymbol{r},t) = \exp\left\{i\left[\boldsymbol{p}\cdot\boldsymbol{r} - \alpha_{\boldsymbol{p}}\cos\omega t - Et - \zeta(t) + \frac{1}{c}\boldsymbol{A}(t)\cdot\boldsymbol{r}\right]\right\}, \quad (2)$$

where

$$E = \frac{p^2}{2}, \quad \alpha_{\boldsymbol{p}} = \frac{\boldsymbol{p}\cdot\boldsymbol{F}_0}{\omega^2}, \quad \zeta(t) = \frac{1}{2c^2}\int_{-\infty}^{t} A^2(t')dt'.$$

If one neglects the laser-field effects on the incoming and outgoing electrons, then the Volkov solution (2) reduces to a usual plane wave,

$$\chi_{\boldsymbol{p}}(\boldsymbol{r},t) = \exp[i(\boldsymbol{p}\cdot\boldsymbol{r} - Et)]. \quad (3)$$

In references [17,18], the plane-wave and Volkov-function treatments were compared and the latter was shown to be necessary to obtain accurate results for the laser-assisted momentum profiles.

The laser-field influence on the ground states of the He atom and He^+ ion is accounted for within first-order perturbation theory. The corresponding expressions are

$$\psi_i(\boldsymbol{r}_1,\boldsymbol{r}_2,t) = e^{-i\mathcal{E}_{\mathrm{He}}t}\left[1 - \frac{\boldsymbol{F}_0\cdot(\boldsymbol{r}_1+\boldsymbol{r}_2)}{\omega_{cl}}\cos\omega t\right] \times \Phi_i(\boldsymbol{r}_1,\boldsymbol{r}_2), \quad (4)$$

$$\psi_f(\boldsymbol{r},t) = e^{-i\mathcal{E}_{1s}t}\left(1 - \frac{\boldsymbol{F}_0\cdot\boldsymbol{r}}{\omega_{cl}}\cos\omega t\right)\varphi_{1s}(\boldsymbol{r}), \quad (5)$$

where Φ_i and φ_{1s} are the unperturbed ground-state wave functions of the He atom and He^+ ion, respectively, $\omega_{cl} \sim |\mathcal{E}_{\mathrm{He}(1s)}|$ is a closure parameter (see, for instance, Refs. [29,30]). A laser-dressed $n = 2$ state of the He^+ ion is constructed from the unperturbed $n = 2$ states:

$$|\psi_f(t)\rangle = \sum_{l=0,1}\sum_{m=-l}^{l} a_{lm}(t)e^{-i\mathcal{E}_{n=2}t}|2lm\rangle. \quad (6)$$

Using the ansatz (6) for the solution of the time-dependent Schrödinger equation, we obtain

$$\psi_{2s}(\boldsymbol{r},t) = e^{-i\mathcal{E}_{n=2}t}\left[\cos\left(\frac{3F_0}{Z\omega}\sin\omega t\right)\varphi_{2s}(\boldsymbol{r}) - i\sin\left(\frac{3F_0}{Z\omega}\sin\omega t\right)\varphi_{2p_0}(\boldsymbol{r})\right], \quad (7)$$

$$\psi_{2p_0}(\boldsymbol{r},t) = e^{-i\mathcal{E}_{n=2}t}\left[\cos\left(\frac{3F_0}{Z\omega}\sin\omega t\right)\varphi_{2p_0}(\boldsymbol{r}) - i\sin\left(\frac{3F_0}{Z\omega}\sin\omega t\right)\varphi_{2s}(\boldsymbol{r})\right], \quad (8)$$

$$\psi_{2p_{\pm1}}(\boldsymbol{r},t) = e^{-i\mathcal{E}_{n=2}t}\varphi_{2p_{\pm1}}(\boldsymbol{r}). \quad (9)$$

If the parameter F_0/ω is small, these equations correspond to first-order perturbation theory.

It can be shown that the FDCS has the form of a sum over processes with different numbers of emitted ($N > 0$) or absorbed ($N < 0$) photons [16]:

$$\frac{d\sigma}{dE_s dE_e d\Omega_s d\Omega_e} = \sum_{N=-\infty}^{\infty} d^3\sigma_N \times \delta(E_s + E_e + \mathcal{E}_f - E_0 - \mathcal{E}_{\mathrm{He}} + U_p + N\omega), \quad (10)$$

where $\mathcal{E}_f$ is the unperturbed final-state ionic energy and $U_p = F_0^2/4\omega^2$ is a ponderomotive potential. The N-photon triple differential cross section (TDCS) is given by

$$d^3\sigma_N = \frac{p_s p_e}{4\pi^3 p_0}\left(\frac{d\sigma}{d\Omega}\right)_{ee}|\mathcal{F}_N(\boldsymbol{q})|^2, \quad (11)$$

where $(d\sigma/d\Omega)_{ee}$ is the half-off-shell Mott-scattering cross section that takes account of exchange between the colliding electrons, and

$$\mathcal{F}_N(\boldsymbol{q}) = \frac{\omega}{2\pi}\int_{-\pi/\omega}^{\pi/\omega} dt\, e^{i(\mathcal{E}_{\mathrm{He}} - \mathcal{E}_f - \frac{q^2}{2} - U_p - N\omega)t} \times \langle\chi_{\boldsymbol{q}}(t)\psi_f(t)|\psi_i(t)\rangle \quad (12)$$

is the laser-assisted momentum profile.

3 Results and discussion

Below, we present and analyze the results of numerical calculations of the momentum profiles for the laser-assisted $(e, 2e)$ processes of helium in symmetric noncoplanar EMS kinematics (see, for instance, Refs. [21,22]). In this kinematics, the scattered and ejected electron angles with respect to the incident electron direction are $\theta_s = \theta_e = 45°$, and the scattered and ejected electron energies are $E_s = E_e = E$. The TDCS is studied as a function of q which is varied by scanning the out-of-plane azimuthal angle of the ejected electron ϕ_e. We consider such a value of the incident electron energy, namely $E_0 = 6$ keV $- \mathcal{E}_{\rm He}$ ($\mathcal{E}_{\rm He} = -2.90356$ a.u.), and such a range of q values that in the absence of the laser field the effects of distortion of the plane waves and the second Born effects are expected to be subsidiary (see Ref. [22] for detail). The following two orientations of the laser electric field are inspected: $\mathbf{F}_0$ is parallel to $\mathbf{p}_0$ (LP$\|$ geometry) and $\mathbf{F}_0$ is perpendicular both to $\mathbf{p}_0$ and to $\mathbf{p}_s$ (LP$\perp$ geometry). Bearing in mind possible experimental realization [19], the laser frequency and intensity are set to be $\omega = 1.55$ eV and $I = 5 \times 10^{11}$ W/cm^2, respectively.

Four different models for the He wave function Φ_i were employed in the present calculations. These are the Roothaan-Hartree-Fock (RHF) function of Clementi and Roetti [31], one of the Silverman-Platas-Matsen (SPM) functions [32], the function of Bonham and Kohl (BK) [33], and a configuration-interaction (CI) function of Mitroy et al. [34]. The RHF function has the form

$$\Phi_{RHF}(\mathbf{r}_1, \mathbf{r}_2) = \varphi(\mathbf{r}_1)\varphi(\mathbf{r}_2),$$

$$\varphi(\mathbf{r}) = \sum_{j=1}^{5} a_j \varphi_{1s}(r, Z{=}\gamma_j) {=} \sum_{j=1}^{5} a_j \left(\frac{\gamma_j^3}{\pi}\right)^{1/2} e^{-\gamma_j r}. \tag{13}$$

It is uncorrelated, giving a total energy of -2.86168 a.u. In contrast, the SPM function takes into account both radial and angular correlations between electrons in helium. It is given by:

$$\Phi_{SPM}(\mathbf{r}_1, \mathbf{r}_2) = \frac{1}{(1+\lambda^2)^{1/2}} \times \Bigg\{ N_{1s}[\varphi_{1s}(r_1, a)\varphi_{1s}(r_2, b) + \varphi_{1s}(r_1, b)\varphi_{1s}(r_2, a)] + \frac{\lambda}{\sqrt{3}} \sum_{m=-1}^{1} \varphi_{2p_m}(\mathbf{r}_1, g)\varphi^*_{2p_m}(\mathbf{r}_2, g) \Bigg\}. \tag{14}$$

The corresponding total energy is $\mathcal{E}_{\rm He} = -2.89523$ a.u.

The BK function is also correlated, having the form

$$\Phi_{BK}(\mathbf{r}_1, \mathbf{r}_2) = N \left[\phi(a, b)(1 + A r_{12} e^{-\lambda r_{12}}) + \phi(c, d)(B + C e^{-\mu r_{12}}) + D\phi(e, f)\right],$$
$$\phi(a, b) = e^{-a r_1 - b r_2} + e^{-a r_2 - b r_1}. \tag{15}$$

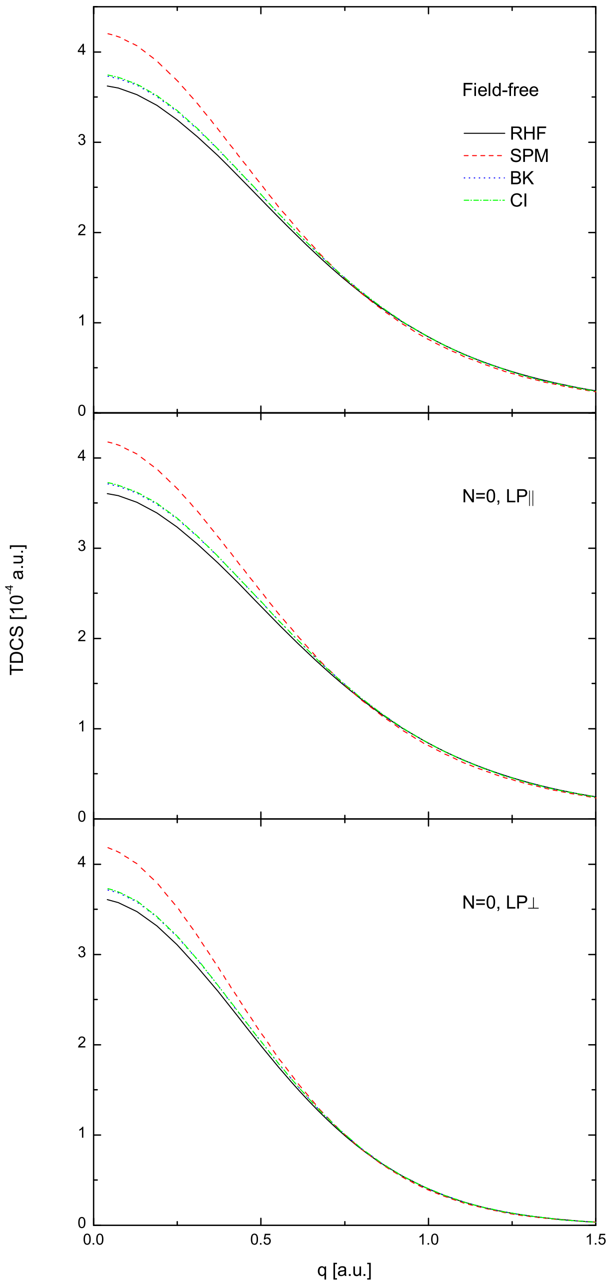

Fig. 1. Field-free and $N = 0$ laser-assisted TDCS, when the He^+ ion is left in the $n = 1$ state.

It gives a total energy of -2.90349 a.u. Finally, the CI wave function is constructed as follows:

$$\Phi_{CI}(\mathbf{r}_1, \mathbf{r}_2) = \sum_{n=1}^{5} \sum_{l=0}^{n-1} N_{nl} P_{nl}(r_1) P_{nl}(r_2) \times \sum_{m=-l}^{l} Y^*_{lm}(\hat{\mathbf{r}}_1) Y_{lm}(\hat{\mathbf{r}}_2), \tag{16}$$

where $P_{nl}(r)$ is the radial part of the natural orbital [35]. The total energy yielded by the CI function is $\mathcal{E}_{\rm He} = -2.90315$ a.u.

First we consider ionization of helium when the residual He^+ ion is left in the laser-dressed $n = 1$ state. Figure 1

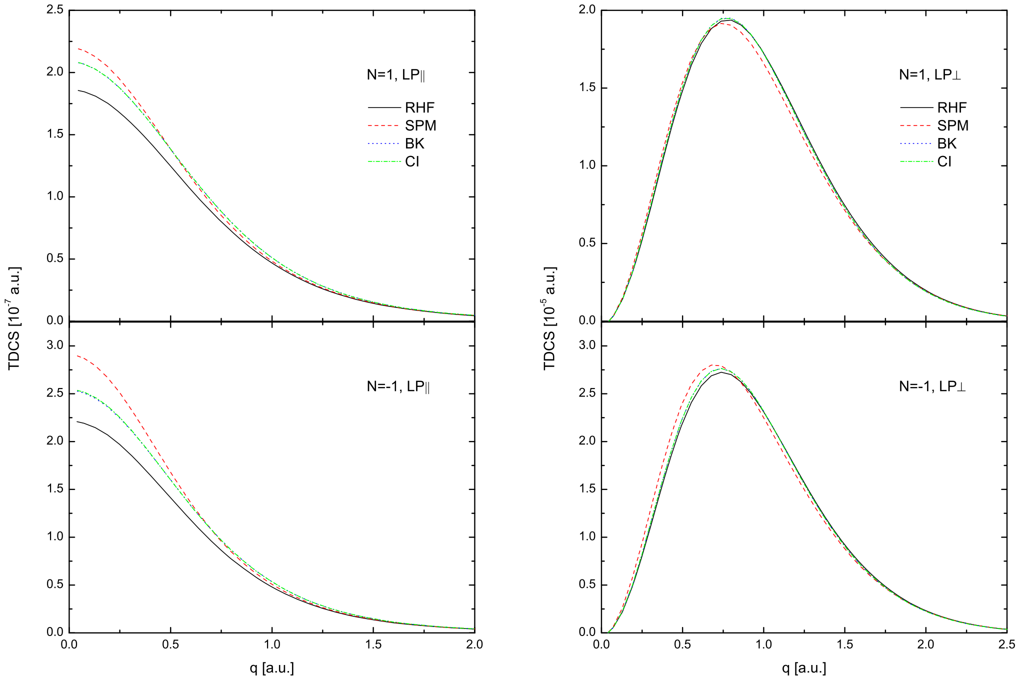

Fig. 2. The $N = \pm 1$ laser-assisted momentum profiles corresponding to the $(e, 2e)$ transition to the $n = 1$ state of He^+.

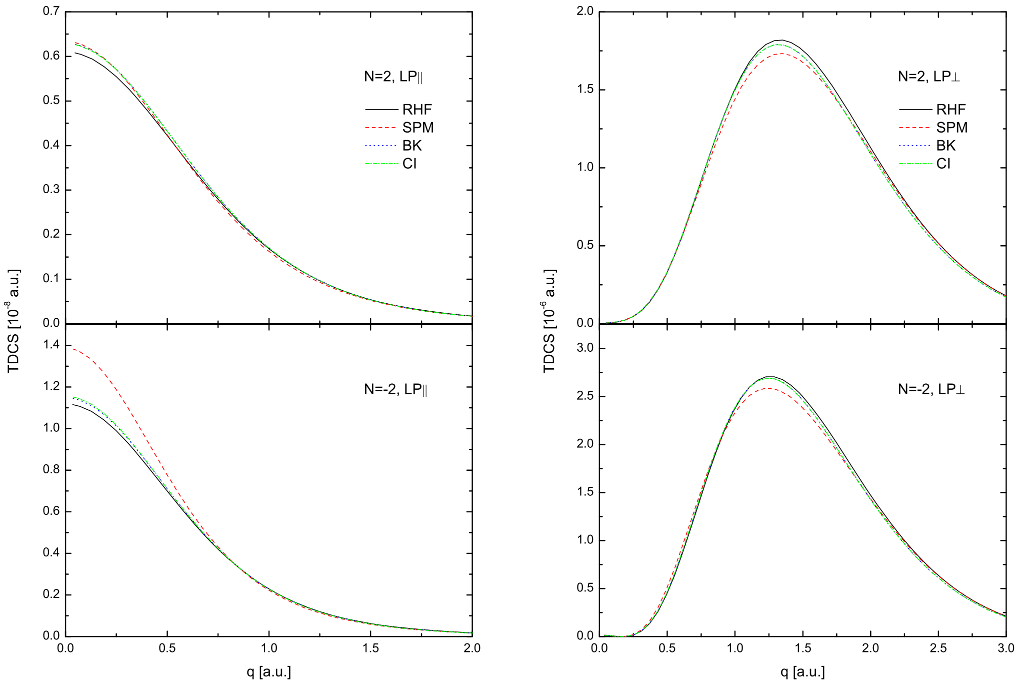

Fig. 3. The same as in Figure 2, but for the $N = \pm 2$ case.

shows how the field-free TDCS corresponding to the $(e, 2e)$ transition to the ground state of He^+ is modified by the presence of the laser field when the total number of photons exchanged between the colliding system and the field is $N = 0$. Typically, the field-free results using different models of the He ground state are close to each other (see also Ref. [21]). In particular, the accurate correlated functions, BK and CI, yield practically identical momentum profiles. The same picture is observed in the case of the laser-assisted momentum profiles presented in Figure 1. The laser-field effect is small in the LP∥ geometry, and it is more or less appreciable in the LP⊥ geometry at large q values, where the laser-assisted momentum profiles notably diminish in magnitude relative to the field-free case.

Figures 2 and 3 show numerical results for, respectively $N = \pm 1$ and $N = \pm 2$ laser-assisted TDCS when

$n = 1$. They are much smaller in magnitude, particularly in the LP$\|$ geometry, than the $N = 0$ ones. This is explained by the low intensity of the laser field – the probability of multiphoton processes rapidly decreases when the number of involved photons increases. It can be seen that in the LP$\perp$ geometry the results using different helium functions are even closer to each other than those in Figure 1. These results also exhibit a qualitatively different q dependence to those in the LP$\|$ geometry, which behave similarly to the momentum profiles in Figure 1. Finally, similar to Figure 1, the BK and CI results are practically indistinguishable.

Let us turn to the case of ionization-excitation. The corresponding field-free and $N = 0$ laser-assisted momentum profiles are shown in Figure 4. As anticipated (see, for instance, Ref. [21]), the field-free momentum profile using the uncorrelated RHF function strongly differs, both in shape and in magnitude, from those using the correlated functions (SPM, BK and CI). The laser field has no appreciable effect, except in the LP$\perp$ geometry at large q values, where the momentum profiles are notably suppressed when compared to the field-free results. And the same as in Figures 1–3, the results using the BK and CI functions are practically identical.

The $N = \pm 1$ and $N = \pm 2$ laser-assisted momentum profiles corresponding to the $(e, 2e)$ transition to the $n = 2$ state of He^+ are shown in Figures 5 and 6, respectively. Similar to the $n = 1$ case, their values are strongly suppressed, particularly in the LP$\|$ geometry, relative to the field-free and $N = 0$ results. Also similar to the $n = 1$ case, they exhibit the same q dependence as the field-free and $N = 0$ results if the LP$\|$ geometry is realized, but behave in a qualitatively different manner in the LP$\perp$ geometry, where they have zeros instead of maxima at small q. The most important finding is that the BK and CI results are not indistinguishable anymore, at least in the LP$\|$ geometry. In particular, in this geometry when $N = -2$, the laser-assisted momentum profile using the CI function appears to be about twice larger in magnitude than that using the BK function.

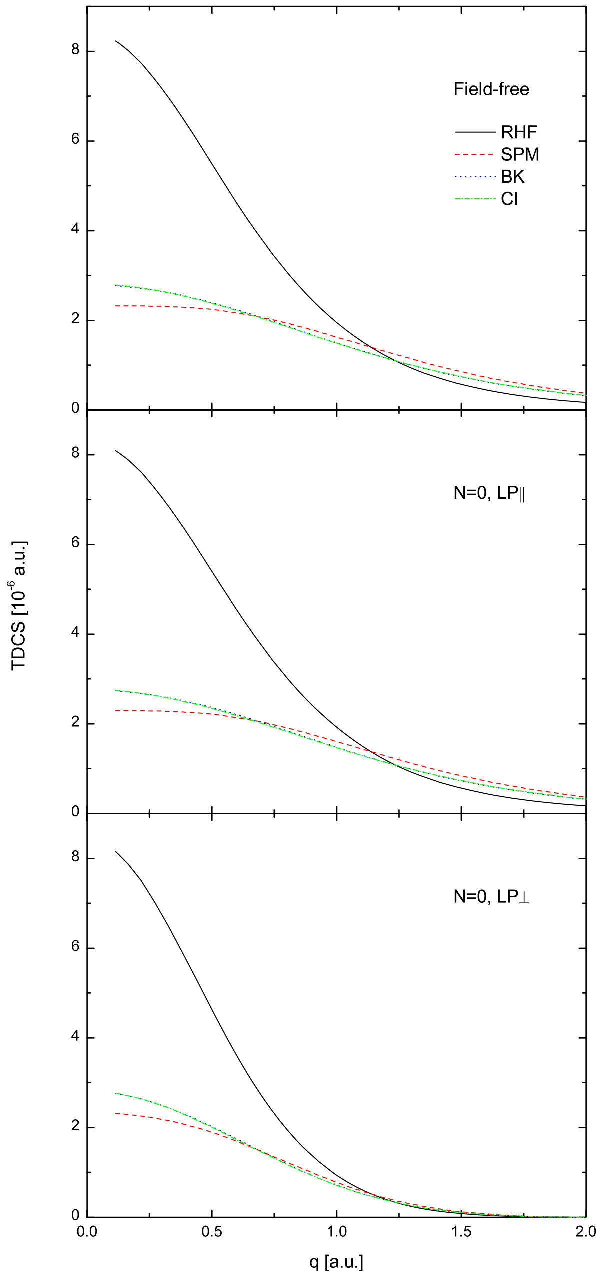

Fig. 4. The same as in Figure 1, but when the He^+ ion is left in the $n = 2$ state.

4 Summary and conclusions

We carried out a theoretical analysis of electron-impact ionization-excitation of He in the EMS kinematics and in the presence of a linearly-polarized laser field, focusing on sensitivity of the laser-assisted momentum profiles to the model of the atomic ground state. For this purpose, we performed numerical calculations for $(e, 2e)$ transitions to the $n = 1$ and $n = 2$ states of He^+ assisted by N-photon processes using different trial wave functions of He. In the case of the laser-field parameters that can be realized in the upcoming measurements [19], we found that the laser-assisted momentum profiles are weakly sensitive to the model of the He ground state when the He^+ ion remains in the $n = 1$ state. In contrast, when the He^+ ion is left in the $n = 2$ state, the results strongly depend on the employed He wave function. Moreover, while the field-free momentum profiles for $n = 2$ using accurate correlated functions are practically identical, the corresponding results in the presence of laser radiation become clearly distinguishable in the LP$\|$ geometry when $N \neq 0$.

The results of the present work show that the laser-assisted EMS method has a rich potential not only for exploring laser effects on electron momentum distributions in various targets but also for studying electron-electron correlations in many-electron atoms. While the low-frequency and low-intensity laser field only slightly influences the atomic bound states, its effect on the fast incoming and outgoing electrons can not be discarded [17,18]. The plane waves are modified by the laser field into the Volkov functions, and thus one obtains a

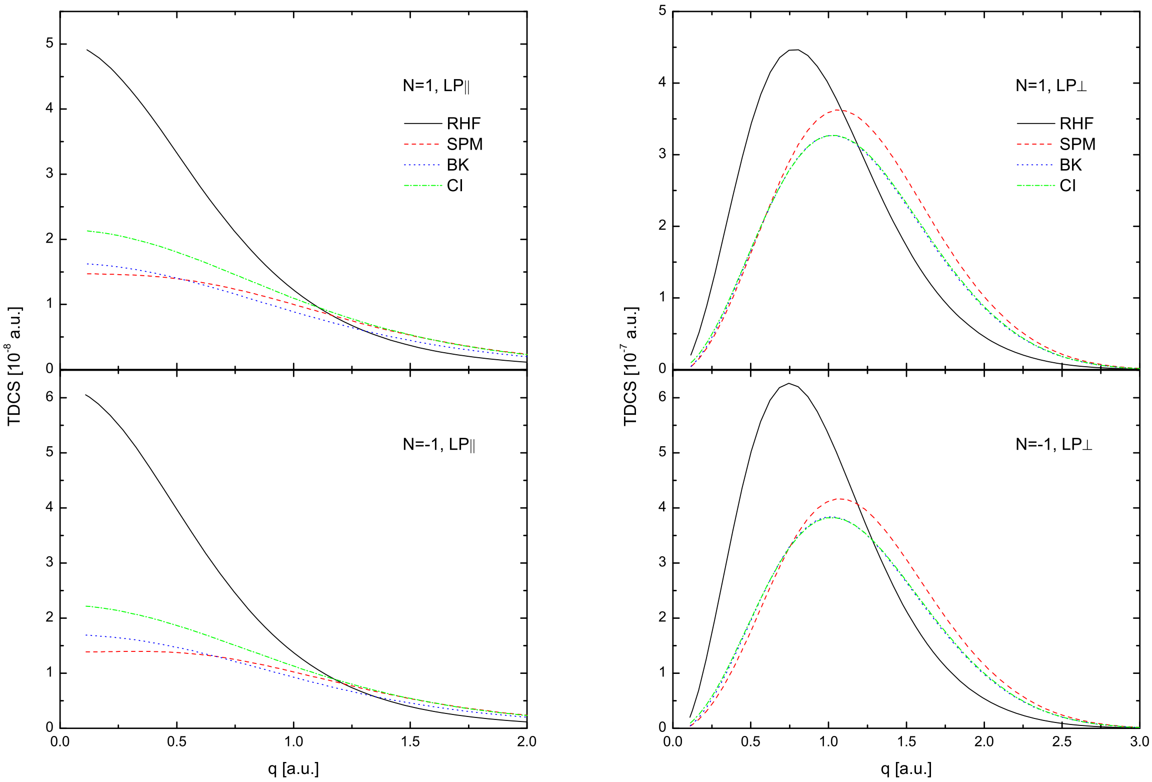

Fig. 5. The same as in Figure 2, but for $n = 2$.

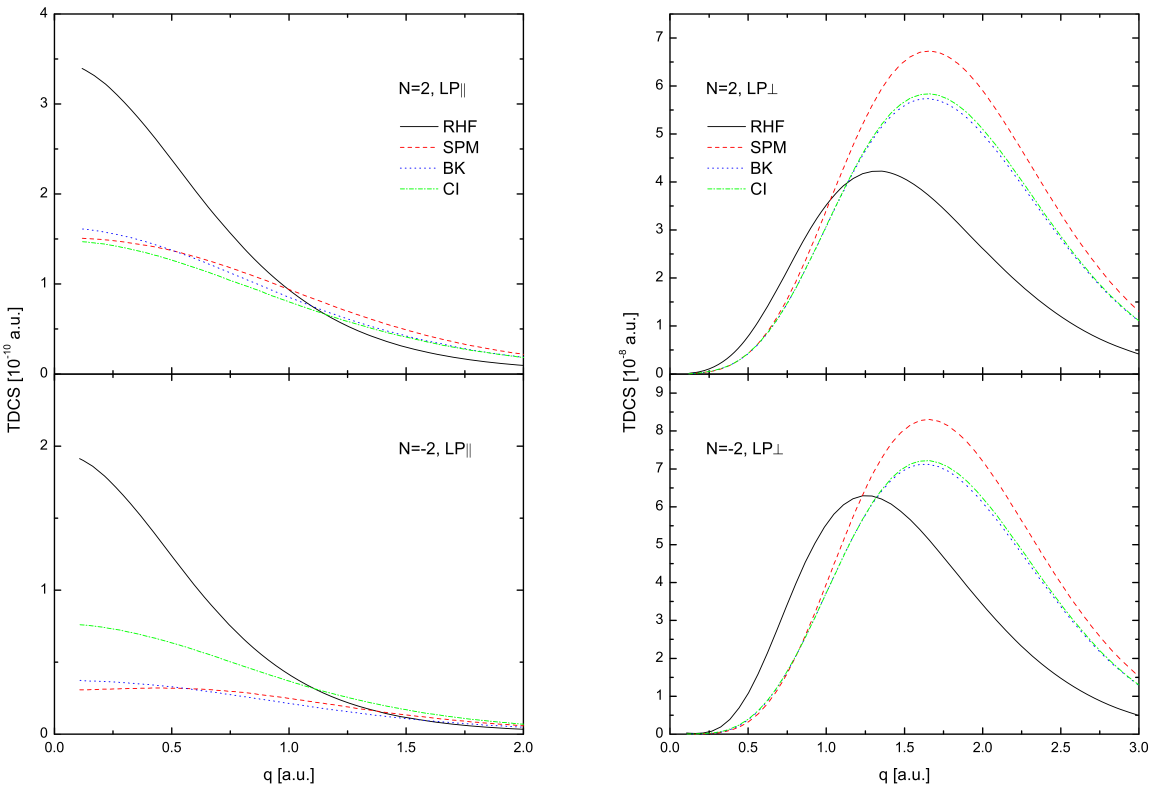

Fig. 6. The same as in Figure 3, but for $n = 2$.

new tool for investigating the Kohn-Sham atomic orbital [2], which is complementary to the usual, field-free EMS method that measures the momentum density of this orbital.

We are grateful to S.I. Vinitsky and O. Chuluunbaatar for useful discussions. This work was supported by the Russian Foundation for Basic Research (Grant No. 14-01-00420-a).

References

1. V.G. Neudatchin, Yu.V. Popov, Yu.F. Smirnov, Phys. Usp. **42**, 1017 (1999)
2. E. Weigold, I.E. McCarthy, *Electron Momentum Spectroscopy* (Kluwer Academic/Plenum Publishers, New York, 1999)
3. M. Takahashi, Bull. Chem. Soc. Jpn **82**, 751 (2009)
4. C.J. Joachain, N.J. Kylstra, R.M. Potvliege, *Atoms in Intense Laser Fields* (Cambridge University Press, Cambridge, 2011)
5. C. Höhr, A. Dorn, B. Najjari, D. Fischer, C.D. Schroter, J. Ullrich, Phys. Rev. Lett. **94**, 153201 (2005)
6. C. Höhr, A. Dorn, B. Najjari, D. Fischer, C.D. Schroter, J. Ullrich, J. Electron Spectrosc. Relat. Phenom. **161**, 172 (2007)
7. F. Ehlotzky, A. Jaroń, J.Z. Kamiński, Phys. Rep. **297**, 63 (1998)
8. F. Ehlotzky, Phys. Rep. **345**, 175 (2001)
9. A. Makhoute, D. Khalil, A. Maquet, R. Taïb, J. Phys. B **32**, 3255 (1999)
10. S.-M. Li, J. Berakdar, S.-T. Zhang, J. Chen, J. Phys. B **38**, 1291 (2005)
11. S.-M. Li, J. Berakdar, S.-T. Zhang, J. Chen, J. Electron Spectrosc. Relat. Phenom. **161**, 188 (2007)
12. A. Chattopadhyay, C. Sinha, Phys. Rev. A **72**, 053406 (2005)
13. S.G. Deb, S. Roy, C. Sinha, Eur. Phys. J. D **55**, 591 (2009)
14. S.G. Deb, C. Sinha, Eur. Phys. J. D **60**, 287 (2010)
15. M.-Y. Zheng, S.-M. Li, Phys. Rev. A **82**, 023414 (2010)
16. K.A. Kouzakov, Yu.V. Popov, M. Takahashi, Phys. Rev. A **82**, 023410 (2010)
17. A.A. Bulychev, K.A. Kouzakov, Yu.V. Popov, Phys. Lett. A **376**, 484 (2012)
18. A.A. Bulychev, K.A. Kouzakov, Yu.V. Popov, Proc. SPIE **8699**, 86991B (2013)
19. M. Yamazaki, Y. Kasai, K. Oishi, H. Nakazawa, M. Takahashi, Rev. Sci. Instrum. **84**, 063105 (2013)
20. J.P.D. Cook, I.E. McCarthy, A.T. Stelbovics, E. Weigold, J. Phys. B **17**, 2339 (1984)
21. N. Watanabe, Y. Khajuria, M. Takahashi, Y. Udagawa, P.S. Vinitsky, Yu.V. Popov, O. Chuluunbaatar, K.A. Kouzakov, Phys. Rev. A **72**, 032705 (2005)
22. N. Watanabe, Y. Udagawa, M. Takahashi, K.A. Kouzakov, Yu.V. Popov, Phys. Rev. A **75**, 052701 (2007)
23. M. Zarcone, D.L. Moores, M.R.C. McDowell, J. Phys. B **16**, L11 (1983)
24. D. Khalil, A. Maquet, R. Taïeb, C.J. Joachain, A. Makhoute, Phys. Rev. A **56**, 4918 (1997)
25. L.V. Keldysh, Sov. Phys. JETP **20**, 1307 (1965)
26. D.H. Kobe, A.L. Smirl, Am. J. Phys. **46**, 624 (1978)
27. D.M. Volkov, Z. Phys. **94**, 250 (1935)
28. M.V. Fedorov, *Atomic and Free Electrons in a Strong Light Field* (World Scientific, Singapore, 1997)
29. S.-M. Li, Z.-J. Chen, Q.-Q. Wang, Z.-F. Zhou, Eur. Phys. J. D **7**, 39 (1999)
30. A.B. Voitkiv, J. Ullrich, J. Phys. B **34**, 1673 (2001)
31. E. Clementi, C. Roetti, At. Data Nucl. Data Tables **14**, 177 (1974)
32. J.N. Silverman, O. Platas, F.A. Matsen, J. Chem. Phys. **32**, 1402 (1960)
33. R.A. Bonham, D.A. Kohl, J. Chem. Phys. **45**, 2471 (1966)
34. J. Mitroy, I.E. McCarthy, E. Weigold, J. Phys. B **18**, 4149 (1985)
35. P.-O. Löwdin, Phys. Rev. **97**, 1474 (1955)